Solidification Microstructure Simulation of Ti-6Al-4V in Metal Additive Manufacturing: A Review

Jinghao Li, Xianglin Zhou, Mathieu Brochu, Nikolas Provatas, Yaoyao Zhao

▶ **To cite this version:**

Jinghao Li, Xianglin Zhou, Mathieu Brochu, Nikolas Provatas, Yaoyao Zhao. Solidification Microstructure Simulation of Ti-6Al-4V in Metal Additive Manufacturing: A Review. Additive Manufacturing, 2020, 31, pp.100989. 10.1016/j.addma.2019.100989 . hal-03628793

HAL Id: hal-03628793
https://hal.science/hal-03628793

Submitted on 2 Apr 2022

HAL is a multi-disciplinary open access archive for the deposit and dissemination of scientific research documents, whether they are published or not. The documents may come from teaching and research institutions in France or abroad, or from public or private research centers.

L'archive ouverte pluridisciplinaire **HAL**, est destinée au dépôt et à la diffusion de documents scientifiques de niveau recherche, publiés ou non, émanant des établissements d'enseignement et de recherche français ou étrangers, des laboratoires publics ou privés.

Solidification Microstructure Simulation of Ti-6Al-4V in Metal Additive Manufacturing: A Review

Jinghao Li[1], Xianglin Zhou[2, *], Mathieu Brochu[3], Nikolas Provatas[4], Yaoyao Fiona Zhao[1, *]

[1]Department of Mechanical Engineering, McGill University, Montreal, Québec, Canada H2A0C3; [2]State Key Laboratory for Advance Metals and Materials, University of Science and Technology Beijing, China 10083; [3]Department of Mining and Materials Engineering, McGill University, Montreal, Québec, Canada H3A0C5; [4] Department of Physics, McGill University, Montréal, Québec, Canada H3A 2T8

Abstract

Metal additive manufacturing (MAM) technology is now changing the pattern of the high-end manufacturing industry, among which microstructure simulation gradually shows its importance and attracts many research interests. As the simulation targets, this paper summarizes the unique microstructure characteristics in MAM fabricated parts, Ti-6Al-4V as an example. Further discussions are focused on the development of solidification microstructure simulation methods as well as their capacity and applicability on MAM. Finally, the difficulties and suggested future research topics in MAM microstructure simulation are addressed.

Keywords: Additive Manufacturing; Microstructure; Simulation; Solidification

1 Introduction

Additive manufacturing (also known as 3D printing) refers to a process by which digital 3D design is fabricated in a layer by layer fashion. Metal additive manufacturing (MAM) methods based on powder, wire, sliced metals and alloys are famous for their flexibility, efficiency, and accuracy [1]. Due to the nature of MAM process, which adds material only at the desired place, the lead-time and material waste are reduced to a relatively low level. More importantly, since the tooling is no longer needed, MAM unlocks a significant amount of constraints for the designers to design products with complex geometry [2]. The technical features of MAM make it suitable for industries with small batch and high complexity part geometry, especially hollow structures and complex curved surfaces. There are already relatively mature applications at present in the area of aerospace, remanufacturing, medical industries and so on. MAM technologies can be roughly divided into two categories, namely, direct energy deposition (DED) and powder bed fusion (PBF). There are several technologies under each category branded by different manufacturers [3, 4]. MAM technologies based on different types of high energy beam (laser and electron beam) are operated under different environment: vacuum environment is needed for the electron beam to travel through and laser can propagate in an inert atmosphere. Also, the cooling rate (product of thermal gradient and solidification rate) in MAM can changes from 10^3 K/s in DED to 10^5 K/s in PBF. The different energy sources, process parameters as well as the cooling conditions in MAM technologies lead to significant differences among the resultant melt pool geometries, which will further influence the fabricated microstructures. Consider the melt pool size alone can change from hundreds of micrometers in PBF to several millimeters in DED. Uncertainties in the process-structure-property (PSP) linkage are restricting the development and application of MAM techniques [5]. Thus, recognizing the interplay between PSP linkage in MAM is crucial for quality control and development of this technology. Modeling approaches and numerical simulations are the ideal tools to fill the gap by saving time and experimental costs [6]. These models enable mechanical property predictions from the process and material parameters and serve as a guideline for design, process control, and optimization.

Corresponding authors.
E-mail addresses: yaoyao.zhao@mcgill.ca (Y.F. Zhao), bkdzxl@gmail.com (X. Zhou)

Among the limited number of printable alloy systems including Ti-based, Fe-based, Al-based, Ni-based and Co-based alloys, MAM technologies inevitably lead to unique microstructural characteristics w.r.t. traditional forming and manufacturing methods. These differences are inevitable results of the melting, solidification and cooling condition provided by MAM, and the material properties including nucleation, grain growth behaviors and solid phase transformation, hence the different resultant mechanical properties and defects. In the past few decades, titanium alloys were found to be suitable for additive manufacturing and attracted a lot of research interest [7]. In this paper, the Ti-6Al-4V alloy is selected to explain the common microstructural characteristics in MAM, including columnar grains, nucleation and epitaxial grain growth behavior as well as the solid phase composition. These characteristics are also frequently observed in other printable alloy systems; most of the materials have all three, and the rest should be investigated individually. In this paper, dendritic columnar grains of as-solidified phases, such as the primary β of Ti-6Al-4V, are simulation targets and referred to as 'grains' or 'column grains' for simplicity.

This work aims to provide a comprehensive review of the state-of-art microstructure simulation methods for MAM fabricated parts to accurately predict the solidification microstructure in terms of grain morphology and texture. These microstructural features can be further applied to mechanical property prediction and process optimization. Existing thermal welding models were found to be inadequate for describing MAM process due to inconsistencies in predictions of the microstructures [8-10]. MAM deposition processes are characterized by rapid, directional solidification due to the layer by layer build-up process, the microstructure and mechanical properties of the deposited materials depend strongly on the cooling condition and subsequent thermo-mechanical cycles. The microstructural characteristics in MAM fabricated alloys are summarized first, where Ti-6Al-4V is selected as an example because it includes all the three microstructural characteristics. Then, the grain scale simulation approaches used to numerically model the solidification process in MAM are discussed in detail and compared w.r.t. their respective capacity and applicability. Finally, the challenges and opportunities in the area of microstructure simulation for MAM are addressed.

2 General Microstructural Characteristics of Ti-6Al-4V in MAM

2.1 Columnar Grains

MAM studies have shown that columnar grain is a common microstructural characteristic in the fabricated samples [7, 11-18]. When considering the cooling condition of melt pool bottom in terms of the thermal gradient (G) and solidification rate (R), the cooling conditions of MAM technologies are mostly located at the columnar zone of G-R diagram [19-21]. The columnar grains frequently observed in MAM fabricated parts tend to elongate along the build direction (e.g., the prior β grain shown in Fig. 1), approximately parallel to the preferentially growing directions of crystals. This is the result of the onset of solidification at 1660°C, where the fusion transfers into crystallographically ordered state phase characterized by body-centered cubic (bcc) crystal structure. However, in most cases of Ti-6Al-4V, the secondary or higher order branches of dendritic column grains merge [22], and the solid-phase transformation eliminates the original grain morphology. To investigate the original solidification microstructure of MAM fabricated Ti-6Al-4V, the electron back-scattered diffraction (EBSD) technique is frequently used [23-30]. The prior β grain can be characterized by the EBSD reconstruction result to provide the crystal orientation information and the approximate grain morphology as well.

The reason for the columnar grains going through multiple layers is the so-called 'epitaxial growth' behavior in MAM [31]. From the energy point of view, it will save more free energy if nucleation starts from partially melted grains in the previous layer rather than generating a new one. The newly formed

Corresponding authors.
E-mail addresses: yaoyao.zhao@mcgill.ca (Y.F. Zhao), bkdzxl@gmail.com (X. Zhou)

grains will inherit crystallographic information like grain orientations and size from existing crystals. Those with the preferentially growing directions align with thermal gradient tend to stand out from the competitive grain growth and develop even bigger through MAM build-up process. Take DED as an example, the column grains can develop into millimeter level [32] which can be recognized by the naked eye because of the different visible light absorption capacity between different crystal orientations and boundaries of the column grains.

In a single weld track of MAM, the β grains tend to tilt towards the scanning direction in order to align their preferred growth direction with the maximum thermal gradient direction. Theoretically, if the columnar grains grow steadily and aligned with the thermal gradient direction, it will result in a curvature of the grain shape because the grain will experience a changing thermal gradient direction along the melt pool tail. However, this kind of grain curvature can also be inhibited due to the constrained solidification among the highly textured grains (preferential growth direction in the build-up direction) and the remelting in MAM.

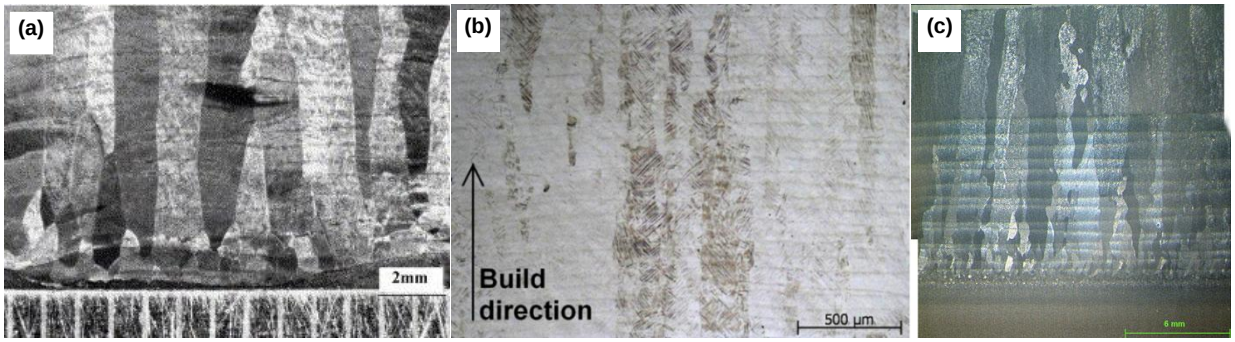

Fig 1: *Column grains in Ti-6Al-4V parts produced by (a) DED [33] (b) Selective Laser Melting (SLM) [34] (c) Gas Tungsten Arc Welding (GTAW) [16]*

Studies have shown that cracks have the propensity to propagate along columnar grain boundaries [35, 36], especially in the build-up direction of MAM where grain boundaries lose their effect of cleavage-cracking resistance [37]. For Ti-6Al-4V, the presence of grain boundary α even accumulate the failure of the material [36]. As a result, the morphology of columnar grains in MAM samples leads to anisotropic mechanical properties in as-built condition [38]. Depending on the loading direction with respect to columnar grain orientation, ductility differences were also discovered in horizontally and vertically built test specimens [23, 25, 36]. To eliminate the unfavorable effect of the column grains, great efforts have been made to achieve the equiaxial grain morphology by investigating the columnar to equiaxed transition (CET) phenomenon with the help of numerical models [12, 39, 40].

2.2 Nucleation and Epitaxial Growth

Nucleation is the first step of the solidification process. In the deterministic models of solidification, the heterogeneous nucleation theory is widely used to explain the small undercooling needed for a conventional solidification process. In the heterogeneous nucleation theory, if the nuclei are simultaneously generated at a critical undercooling value, it is unable to account for the grain density changes in different cooling conditions. This is contrary to observation, where the grain size will decrease drastically at a higher cooling rate. Currently, the instantaneous nucleation theory is broadly accepted by researchers and has been implemented in solidification microstructure simulation where the nucleation phenomenon is considered as a thermally-activated process, and the nuclei density increased by supercooling under a log Gaussian distribution. This can be expressed as the following equation [41]:

Corresponding authors.
E-mail addresses: yaoyao.zhao@mcgill.ca (Y.F. Zhao), bkdzxl@gmail.com (X. Zhou)

$$\frac{dn}{d(\Delta T)} = \frac{n_{max}}{\Delta T_\sigma \sqrt{2\pi}} \frac{1}{\Delta T} \exp\left[-\frac{1}{2}\left(\frac{ln\Delta T - ln\Delta T_0}{\Delta T_\sigma}\right)^2\right] \quad (1)$$

where n_{max} is the total nucleus number per unit volume, ΔT_σ and ΔT_0 are the standard deviation and mean value of the log of supercooling respectively.

In term of nucleation behavior in MAM, epitaxial growth is a common phenomenon. For example, a single crystal can run through multiple layers of material deposition in DED fabricated Ti-6Al-4V samples [17]. In some cases, the column grains even grow throughout the entire length of the printed part. If we consider the partially melted crystal as the substrate for nucleation to start, there will be perfect compatibility between the solid and the liquid phases. Theoretically, there is no nucleation energy barrier, and the wetting angle is zero. It means there are little or no newly formed nuclei in the material deposition process. Thus, the instantaneous nucleation can also be neglected, and the column grains directly epitaxially grow from a crystallographic orientation and grain geometry defined substrate in many MAM solidification microstructure simulations.

However, external factors such as impurity, defects, recrystallization and unmelt metal powders are the main reason for new nuclei in MAM. Take selective laser melting (SLM) which is a type of laser powder bed fusion (LPBF) process as an example, the smaller melt pool compared to DED will inevitably lead to unmelt or half melt powders. These unmelt powder, especially at the contour of the fabricated part, will provide additional nucleation position and change the microstructure dramatically.

2.3 Phase Composition

In Ti-6Al-4V MAM studies, as-built SLM microstructure is composed of the martensitic α' phase with little α or β phases present [34, 42, 43]. The heat input in the DED processed samples usually is higher than that in SLM; thus, the relatively slow cooling rate gives the opportunity for diffusion-controlled solid phase transformation. This results in the α phase forming at the grain boundary of prior β grains (shown in Fig. 2 a-b). The thermal cycles in MAM process usually result in a changing phase composition along the build-up direction. Various solid phase composition conditions along with the newly added deposition layers can be depicted as position-dependent microstructural "maps" (Fig. 2 c) based on known relationships from the thermal history and microstructural evolution.

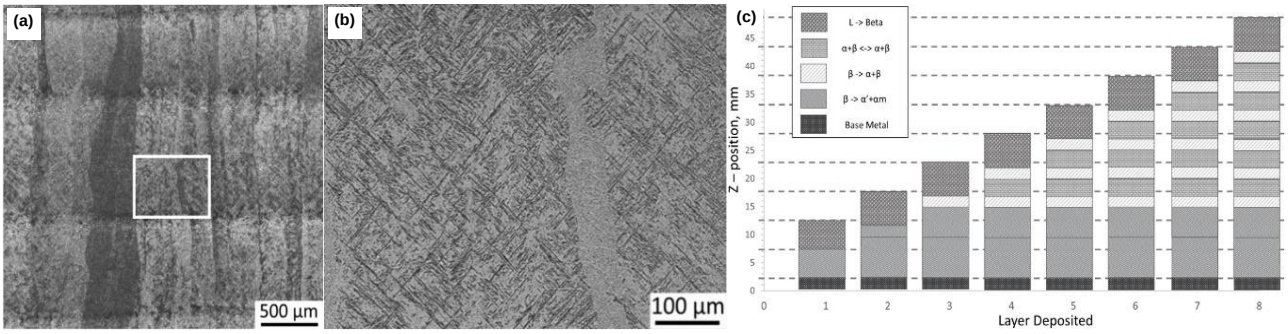

***Fig 2**: Phase Composition of Ti6Al4B fabricated by DED: (a-b) Micrographs of macrostructure and fine microstructure of DED sample [44] (c) Microstructural evolution map of the build as each layer is deposited (reproduced from [38, 45, 46])*

Studies also show that primarily α' microstructure results in low ductility, and the size of α colony is also a determining factor for the mechanical properties [47]. By applying post-process heat treatments to decompose α' into microstructures consisting of α and β phases (i.e., lamellar microstructure), ductility can be improved significantly [34]. Beside Ti-6Al-4V, post-processing and heat treatment are also powerful tools for MAM fabricated alloy systems to control their solid phase composition and mechanical properties [14].

Corresponding authors.
E-mail addresses: yaoyao.zhao@mcgill.ca (Y.F. Zhao), bkdzxl@gmail.com (X. Zhou)

3 Review of Solidification Microstructure Simulation Methods in MAM

The microstructure in a crystal material is a sum up of the thermodynamic non-equilibrium lattice defects compared to an ideal single crystal [48]. These lattice defects usually form detectable patterns that can be used to explain the material properties. One principal aim of material science is to relate macroscopic sample behavior to microstructure [47] quantitatively, and simulation is a good option to bridge the gap. Following this, a microstructure simulation is not necessarily carried out in microscale as long as its simulation target is the microstructure. For all the metal solidification processes including MAM, microstructure simulation can be roughly divided into macroscale (solid state phase transformation, concentration field, etc.), mesoscale (grain texture) and microcosmic (nucleation and grain growth) scale. Furthermore, with the aid of advanced analytic capabilities of the supercomputer, nucleation behaviors are simulated at atomic-scale [49, 50].

Melt pool models in welding have been used as a guide for the development of MAM process and solidification microstructure simulation [51-54]. Factors such as the solidification front velocity, temperature gradient, melt pool shape, travel speed, undercooling, and alloy constitution are vital in the solidification process of MAM to determine the cooling conditions and resultant solidification microstructure in a single melt pool [55]. Extensive literature has documented the polycrystalline microstructures as well as the significant differences in the resulting mechanical properties of MAM components [56-59]. However, due to the rapid development of MAM techniques, it is recognized that matching detection and simulation system are becoming increasingly important [60-64].

The study of dendritic growth and features of crystal grain is another prominent fundamental research topic in solidification microstructure modeling and simulation. It provides a better understanding of the solidification process and resultant microstructure. In the modern sense of solidification microstructure simulation, physical models act as the foundation providing a formal description of the crystal nucleation and grain growth behavior. Microstructural information such as grain size and morphology are gathered under different algorithms through the numerical simulation and implemented on computer visualization. With the rapid development of computer technology, some established macro-transmission models have been used to describe the transport phenomenon and movement of solid-liquid interfaces in space and in time [65]. From these models, temperature and other field data can be extracted and used in the subsequent steps of microstructure simulation. Currently, there are four conventional methods used in the field of solidification microstructure simulation, namely Cellular Automata (CA), Phase Field (PF), Monte Carlo (MC) and deterministic method. The deterministic method is based on solidification kinetics, usually with clear physical implications and application background. However, due to its oversimplification and exclusion of stochastic factors, it can rarely reflect the solidification phenomenon such as nucleation orientation and competitive grain growth. In this work, the first three probabilistic methods are discussed in the following sections.

The blooming of microstructure simulation on MAM, especially in the last decade, is a result of the rapid development of MAM technologies and the simulation methods. Compared to casting, MAM provides more opportunities for cooling condition controllability by manipulating the process parameters in a much smaller region. Simulation increasingly reveals its importance in this area to hit the target of quantitative control on the MAM fabricated microstructure. From all the reviewed solidification microstructure simulation methods shown in table 1, CA is currently the most used method for MAM processes with relatively low computational cost, and it provides the information of rough outline of solidification grain structures. It has also been widely implemented in MAM related topics to investigate the PSP linkage. Under the help of the macro-transmission models, CA method can be launched in 3D level with a scope of multiple layers.

Corresponding authors.
E-mail addresses: yaoyao.zhao@mcgill.ca (Y.F. Zhao), bkdzxl@gmail.com (X. Zhou)

PF methods are capable of high accuracy and resolution in the representation of physical models. It can capture subgrain features in the solidification microstructure, such as secondary or higher order dendrites. However, there is no "free lunch". PF models are usually computationally expensive and can only generate one or a limited number of grains in the simulation region. Extension of PF method to 3D models renders the level of computational resources required prohibitive. Other challenges arise when modelling rapid solidificstion. Specirically, it is not well accepted how to map the asymptotic interface dynamics of PF models onto appropriate non-equilibrium kinetics that incorporate solute trapping and drag; indeed, it is not even well known what the kinetics at the interface should be when solidifiation rates become as high as they do in rapid solidification. For example, it is typically assumed that the contionuous growth model of Aziz and co-workers holds at rapidly moving interfaces [66]. However, there is also compleling evidence from Molecular Dynamics (MD) that the non-equiliubium two-time kinetics of Sobolev and other workers holds at rapidly moving interfaces. The existene of an interface in PF models naturtally leads to the phenomenology of solute trapping and drag [67]. However, the degree of trappiung and drag exhibited by each PF model depends on the size of interface, the interpolation fucntions used, both of whose effects can couple to the rate of solidificsiton. Recent phase field models have considered how to consistently and quantitativley integreate non-equilibrium effects into PF models [68-70].

As for MC method, it is simple and effective in simulating grain growth behavior, especially the recrystallization, but it can only provide the result after a large number of 'trial and error'. In the kinetic Monte Carlo (KMC) simulations for MAM, the subgrain microstructure such as cells and dendrites are simplified, in some cases, even the crystal orientations are neglected. Thus, the competitive grain growth behavior described by this method has a relatively weak physical background compared to CA and PF methods.

CA and KMC methods usually combine with the thermal history sources to predict the microstructure evolution during the solidification process. The thermal history source data normally come from the well-developed macro-transmission models based on finite element, finite difference, or Lattice Boltzmann method. However, PF models are mostly carried out under the 'frozen temperature' assumption, which is only valid under an extremely small region.

Experiments validate most of the simulation results in the reviewed works in terms of grain structure, size, orientation, and texture. Because of PF method's capacity on capturing subgrain microstructural features, dendrite arm spacing is frequently measured in the validation of PF models to compared with the simulation result. However, only a limited number of CA and PF models would validate the melt pool geometry before launching the solidification microstructure simulation. The accuracy of the simulation result is thus discredited by using a non-validated boundary condition.

The computation efficiency is usually an issue to consider when a solidification microstructure simulation is launched in 3D level or multiple layers' region in MAM. Parallel computation is widely applied to arrange the computation task into a multi-core Central Processing Unit (CPU) or Graphics Processing Units (GPU) to increase the processing speed. To save the memory space: iterative data reuse and dynamic allocation strategies are used in CA method; for PF method, this can also be achieved by deriving new evolution equations.

Along with the progress and development of microstructure simulation, new methods, theories, and techniques continuously come forth — for example, the needle-network method which has already shown potentials of its further application in MAM process.

Corresponding authors.
E-mail addresses: yaoyao.zhao@mcgill.ca (Y.F. Zhao), bkdzxl@gmail.com (X. Zhou)

Table 1: Solidification Microstructure Simulation Methods in Grain Level

Simulation Method	Simulation Objective	Dimension	Scope	Thermal History Source	Experimental Validation Method	Computational Efficiency Improve Strategy	Reference
Cellular Automata	Melt Pool Solidification	3D	Multiple Layers	Finite Volume	EBSD Measurement	--	[71]
				Analytical Solution	EBSD Measurement	Parallel computations	[72]
				Finite Difference	Grain Structure and Geometry Analysis	--	[73]
				Finite Element	Grain Structure and Size	Iterative Reuse of Thermal Field Data	[74]
			Single Track	Finite Element	--	Parallel Computations	[75]
				Finite Element and Finite Volume	EBSD Measurement	--	[76]
				Finite Element	Grain Structure	--	[77]
			Melt pool	Analytical Solution	Comparison of Primary Dendrite Arm Spacing	--	[78]
				Thermal– Computational Fluid Dynamics (CFD)	Observations from Literature	--	[79]
			Constant Thermal Gradient Area	Frozen Temperature Approximation	--	--	[80]
		2D	Multiple Layers with Powder	Lattice Boltzmann	Grain Structure and Texture	--	[81]
				Lattice Boltzmann	Grain Size and Texture	--	[64]
			Multiple Layers	Finite Element	Grain Structure and Size	--	[82]
				Finite Difference	Grain Structure and Texture	--	[62]
				Phase Filed Model	Grain Structure and Texture	--	[60]
				Finite Element	Grain Size Measurement	--	[63]
				Finite Element	Grain Structure	--	[83, 84]
			Single Crystal	Lattice Boltzmann model	--	Avoids Large Equation Systems	[85]
	Casting or Directional Solidification	3D	Ingot	Finite Element	Temperature Field Measurement	--	[86]
				Finite Element	Grain Structure	Dynamic Allocation	[87]
				Finite Element	--	Parallel Computations	[88]
				Finite Element	--	--	[89]
			Constant Thermal Gradient Area	Finite Element	Primary Dendrite Spacing	--	[90]
		2D	Section of Ingot	Isothermal	Grain Structure	--	[91-93]
Phase Field	Melt Pool Solidification	3D	$0.65 \times 0.65 \times 10.0$ μm^3	Frozen Temperature	Grain Structure and Primary Dendritic Arm Spacing	--	[94]
			$1 \times 1 \times 2.4$ μm^3	Finite Element (Frozen	--	--	[95]

Corresponding authors.
E-mail addresses: yaoyao.zhao@mcgill.ca (Y.F. Zhao), bkdzxl@gmail.com (X. Zhou)

				Temperature Approximation)			
		2D	Multiple Layers	Phase Filed Model	Observations from Literature	Formulation of New Free Energy Expression	[96]
			Single Track	CFD	Grain Structure and Segregation Analysis	--	[97]
			6 mm × 12 mm	Finite Element	Grain Structure and Arm Spacing Measurement	--	[98]
			150 μm × 150 μm	Lattice Boltzmann	--	--	[99]
			50 μm × 50 μm	Finite Element	Grain Structure and Dendritic Arm Spacing	--	[100]
			12 μm × 12 μm	Frozen Temperature	Grain Structure and Primary Dendritic Arm Spacing	--	[101]
			12 μm × 32.4 μm	Frozen Temperature	Grain Structure and Primary Dendritic Arm Spacing	--	[102]
			150 μm × 100 μm	Analytical Solution	Dendrite Arm Spacing from Literature	--	[103]
	Casting or Directional Solidification	3D	3.072 × 3.078 × 3.072 mm^3	Analytical Solution	--	GPU and Parallel Computation	[104]
			768 × 768 × 768 μm^3	Frozen Temperature	Grain Structure	Parallel Computation and Asynchronous Concurrent Algorithm	[105]
			1.6 × 1.6 × 1.7 mm^3	Analytical Solution	Grain Structure	--	[106]
			1.058 × 1.058 × 1.058 mm^3	Frozen Temperature	--	New Evolution Equation	[107]
		2D	600 μm × 600 μm	Frozen Temperature	Grain Structure	--	[108, 109]
			2 mm × 1.2mm	Frozen Temperature Profile	In Situ X-Ray Imaging	--	[110]
			5 μm - 5mm	Frozen Temperature or Analytical Solution	Grain Structure	--	[111-118]
Monte Carlo	Melt Pool Solidification	3D	Multiple Layers	CFD	Grain Structure and EBSD	--	[119]
			Single Track	CFD	Grain Structure and Melt Pool Geometry	--	[120-122]
		2D	Multiple Layers	CFD	Grain Structure, Orientation and Melt Pool Geometry	--	[123, 124]

Corresponding authors.
E-mail addresses: yaoyao.zhao@mcgill.ca (Y.F. Zhao), bkdzxl@gmail.com (X. Zhou)

3.1 Cellular Automata (CA) Method

CA is a type of algorithm reflecting the states of a collection of cells based on transformation rules, the complex evolution of investigated area in discrete space happens automatically when the rules are applied iteratively. The conventional CA uses local rules where the instantaneous state/value of cellular is a function of its neighbors. Recently, variants of CA method also consider intermediate or long-range interactions [125]. Even though each cellular consists of many identical simple components, together, they are capable of complex behavior and can be used to simulate complex problems [126]. Unlike general dynamics models, CA is not strictly defined by physical equations, but by rules constructed with a set of models [127].

Typically, A CA model is composed of the cell, cellular state, cellular space, cellular neighbors, the function of rule and time. The local interaction between the cell and its neighbors (different types of neighbor algorithms are developed) is specified through deterministic or stochastic transformation rules. Considering two time steps of a one-dimensional CA as an example, the evolution of the model can be simply expressed as [125]:

$$\xi_j^{t_0+\Delta t} = f\left(\xi_{j-1}^{t_0-\Delta t}, \xi_j^{t_0-\Delta t}, \xi_{j+1}^{t_0-\Delta t}, \xi_{j-1}^{t_0}, \xi_j^{t_0}, \xi_{j+1}^{t_0}\right) \quad (2)$$

where ξ is the state variable of a cellular, j is the location subscript, t_0 is the time superscript, and Δt is the time step. The value of an arbitrary state assigned to cellular at a time $(t_0 + \Delta t)$ is determined by its present state ($\xi_j^{t_0}$) and/or its last states ($\xi_j^{t_0}$, $\xi_j^{t_0-\Delta t}$, etc.) together with the states of its two neighboring cells.

When dealing with complex, dynamic and random questions, CA has significant advantages due to its flexible definition of neighbor and action rules. Its application is not limited to a specific area. Now, CA has been used to develop simulation models for sociology, ecology, computer science, physics, chemistry and other subjects [126, 128, 129].

In the past 25 years, CA has successfully been used into microstructure simulations, for example, the static recrystallization [130-134], the dynamic recrystallization [135, 136] and the grain growth behaviors [62-64, 77, 137]. The first CA model to incorporate the solidification behavior was developed in the 1990s [91]. These CA models, initially developed in 2D, was later extended to 3D and coupled with finite element (FE) heat flow calculations resulting in the so-called Cellular Automaton-Finite Element (CAFE) models [41, 87, 91, 138-141]. They are widely applied in investment casting [139], directional solidification [87] and an extensive range of microstructure evolution phenomenon including dendrites, micro-segregation, defects in different alloy systems [22, 142-149]. Also, different kinds of defect formation in casting production process during the last stage of solidification are controlled by CA simulations to achieve the desired microstructure [142]. With the rapid development of MAM, CA method is also widely applied in the solidification microstructure simulations for MAM. For example, the CA method was used in a 2D numerical model to simulate the evolution of solidification grain structure during the laser additive manufacturing process in multiple layers (Fig. 3a). The influence of the different heat source parameters on the resultant microstructure was also investigated [62].

Corresponding authors.
E-mail addresses: yaoyao.zhao@mcgill.ca (Y.F. Zhao), bkdzxl@gmail.com (X. Zhou)

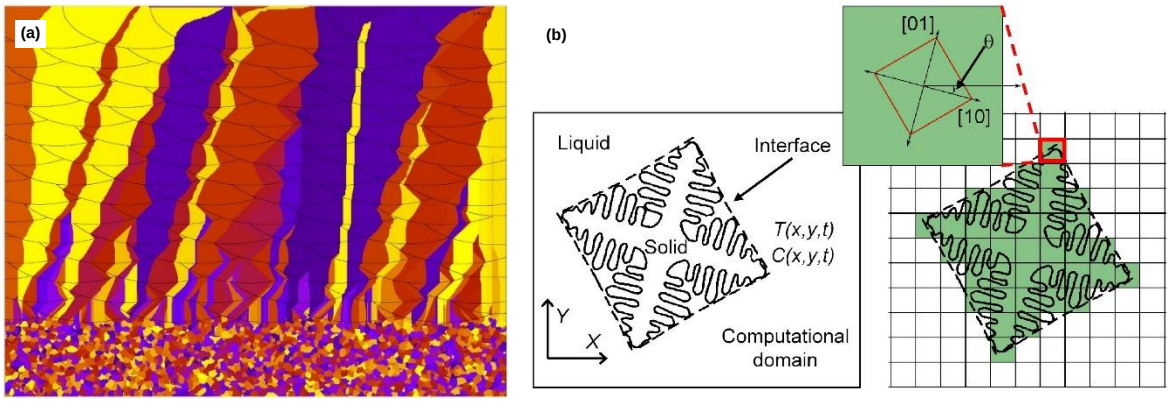

Fig 3*: An example of 2D microstructure simulation using CA method: (a) SLM process which involves multiple layers of material deposited on a polycrystalline substrate (b) Schematic of a single dendritic grain growth in the melt (left) and its CA representation (right). [62]*

In term of solidification microstructure simulation, a CA model is usually achieved by short-term relations or local rules. Every single grain defined by a specific crystal orientation and a nucleation position can develop by its own, and this self-organized behavior will depict the grain boundary geometry as a result of the competitive grain growth.

The physical-based CA models predict the competitive grain growth behavior and interactions between the grains under the dendrite tip growth kinetics. In the area of fusion zone and mushy zone, the total supercooling of a dendrite tip, ΔT, is the sum of four contributions

$$\Delta T = \Delta T_{th} + \Delta T_c + \Delta T_k + \Delta T_r \quad (3)$$

Where ΔT_{th} is the pure thermal undercooling for fluctuation of temperature at solid/liquid interface caused by thermal diffusion, ΔT_c stands for the undercooling contributions associated with solute diffusion, ΔT_k is the kinetic supercooling influenced by the rate at which atoms attach to the solid phase, and it will be significant only if the interfacial growth rate is in the order of 1m/sec, ΔT_r is the curvature supercooling due to curvature of the solid-liquid interface, also called Gibbs-Thomson supercooling. Based on the solidification situation, some contributions on the RHS of equation (3) are neglected in different cases. Then, the growth rate of both columnar and equiaxed grains is calculated as a function of supercooling with the aid of the KGT model [150]. The dendrite tip grain growth rate V_{tip} and its undercooling are related by using the solute supersaturation, Ω, as an intermediate variable under Ivantsov function of the solute Peclet number: $Iv(Pe)$. The relationship between dendrite tip growth rate and undercooling can finally be expressed as

$$V_{tip}(\Delta T) = \frac{D_L}{5.51\pi^2(-m(1-k)^{1.5})\Gamma}\left(\frac{\Delta T^{2.5}}{{C_0}^{1.5}}\right) \quad (4)$$

where V_{tip} is the dendrite tip growth velocity, D_L is the solute diffusion coefficient in the liquid, m is the liquidus slope, k is the partition coefficient, Γ is the Gibbs-Thomson coefficient, C_0 is the initial concentration, detailed derivation can be found in [151]

Corresponding authors.
E-mail addresses: yaoyao.zhao@mcgill.ca (Y.F. Zhao), bkdzxl@gmail.com (X. Zhou)

It should be emphasized here that the dendrite tip growth kinetics we derived above only consider the supercooling contributed by the solute diffusion (ΔT_c). In the case of MAM, the cooling rate is in the order of 10^5 K/sec and it usually leads to an enormous supercooling. So, the influence of supercooling due to grain tip curvature (ΔT_r) and kinetic supercooling are significant and cannot be neglected.

The crystal structure is another aspect which influences the dendrite geometry significantly [152, 153]. To reflect the preferential growth direction of grains (e.g., the <001> directions of prior β in Ti-6Al-4V), Gandin and Rappaz [140] developed the decentered square growth technique in CA method. The algorithm was then improved by Wang and Peter D. Lee to adapt coarser grids with a concomitant loss in resolution [90]. By using the decentered square growth algorithm, the crystallography symmetry and the orientation information are stored in each cell of the grain growth area (Fig. 3 b). Subsequently, the grain cells are capable of growing faster in their preferential growth directions according to the total supercooling and reflect the competitive grain growth behavior quantitatively.

3.2 Phase Field (PF) Method

PF method is a powerful computational approach to solve interfacial problems, such as micro and mesoscale crystal morphology and microstructure evolution [154]. It is widely applied in the research topics such as solidification [106, 114-116, 155], microstructure evolution [156, 157], grain growth [103, 112, 158], dislocation [159], crack propagation [160] and so on.

PF method is a continuum description of the free boundary problem which allows the interface to be smeared over a diffuse region for numerical expedience [161]. Order parameters representing the diffused interface can be used to locate the position of arbitrary and highly non-linear interfaces with out explicitly tracking them. This avoids the difficulties lead by the sharp interface descriptions (maximum velocity, marginal stability, microscopic solvability, interfacial wave) [162-165] in terms of topological complexity, phenomenon descriptions and so on.

In PF models, both the compositional/structural domain and the interface are described by a set of conserved and non-conserved field variables. Governed by Cahn-Hilliard [166, 167] nonlinear diffusion equation and the Allen-Cahn relaxation equation, the field variables are continuous across the interfacial regions, and hence the interfaces in a phase-field model can be diffused to avoid the problem of meshing there highly non-linear interfaces. This strategy can also be understood as metallurgical derivatives of the theories of Onsager and Ginzburg-Landau [125, 168]. In the phase field theory (diffuse interface), the total free energy can be described by

$$F = \int \left[f(c_1, c_2, \dots, c_n, \eta_1, \eta_2, \dots, \eta_n) + \sum_{i=1}^{n} a_i (\nabla c_i)^2 + \sum_{i=1}^{3} \sum_{j=1}^{3} \sum_{k=1}^{p} \beta_{ij} \nabla_i \eta_k \nabla_j \eta_k \right] d^3 r + Gr - r' d3r d3r' \quad (5)$$

where F is the total free energy of an inhomogeneous microstructure system, f is the local free-energy density, G is the function of the long-range interactions, a_i and β_{ij} are the gradient energy coefficients, $c_{1\dots n}$ are conserved field variables, $\eta_{1\dots n}$ are non-conserved field variables [169].

In equation (5), the gradient energy terms come into play at and around the interfaces, and contribute to the total free energy. The way to treat the contribution from various terms to the total free energy is the main differences among different PF models [161, 170].

Crystallographic structures in metal are always representing a highly ordered phase in the format of body-center cubic (bcc), face center cubic (fcc) and hexagonal closed-packed (hcp). For

Corresponding authors.
E-mail addresses: yaoyao.zhao@mcgill.ca (Y.F. Zhao), bkdzxl@gmail.com (X. Zhou)

instance, the Ti-6Al-4V represents a bcc structure after the first order transformation from liquid to its β phase. In a two-dimensional PF model, the fourfold surface energy anisotropy at the solid-liquid interface of a cubic system crystal can be given by

$$a(\theta) = 1 + \varepsilon \cos(4\theta) \tag{6}$$

where ε is the strength of anisotropy and θ is the interface normal direction [101].

When PF models are used to describe the crystalline materials, the basic principle is to use a free energy functional which is minimized by periodic density to represent the periodic and symmetrical nature of a crystal lattice [157]. PF method is also capable of simulating crystal grains with different orientations by introducing multiple order parameters, one for each orientation. An interaction term in the model can be tuned to control coalescence and grain boundary energy during the solidification process. However, the large number of crystal orientations also leads to an equal quantity of order parameters, which increases the computational cost. Due to the extensive computer power required by PF method, there is a limited number of PF model implemented in a melt pool level, let along the whole MAM process. To solve this problem, considerable progress has been made in recent years to increase the efficiency of PF method: In order to keep the numerical scheme of PF model efficient, a new formulation of free energy was derived in [96], and the solidification microstructure simulation was carried out in a region of multiple layers. [107] introduced the nonlinearly preconditioned quantitative PF formula to solve the evolution equations on a computational mesh coarser than those in the conventional method. The quantitative simulations of a large number of dendrites growth are carried out on the scale of centimeters. Parallel computing using GPU is another way to unchain the length scale limitation of PF, in [105], the problem of insufficient GPU memory was circumvented by employing an asynchronous concurrent algorithm. The competitive grain growth behavior was also studied in a 3D PF model under different crystal orientations (shown in Fig. 4).

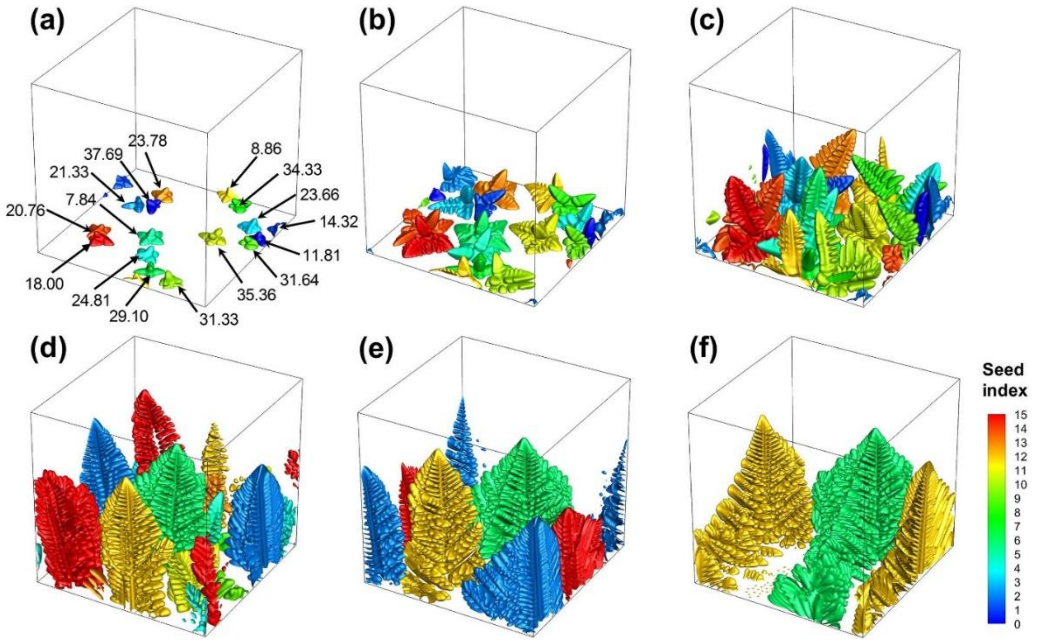

Corresponding authors.
E-mail addresses: yaoyao.zhao@mcgill.ca (Y.F. Zhao), bkdzxl@gmail.com (X. Zhou)

***Fig 4**: PF simulation on dendrite morphology evolution along with solidification time, colors indicate dendrites with different orientations. [105]*

To represent the periodic structure of metal crystals in the atomic scale, an extension of PF method is introduced and known as the phase-field crystal (PFC) method [171]. It describes the evolution of the atomic density of a system according to dissipative dynamics driven by free energy minimization. In PFC approach, solid phase free-energy density is also constructed to be minimized by periodic density states with crystal symmetries. PFC models are derived directly from, and thus inherits some of, the principles of classical density functional theory. So, it is still an atomic-scale model in space. On the other hand, its parameterization is not fully quantitative, which also hinders its application in practical problems including MAM.

3.3 Monte Carlo (MC) Method

MC simulations involve the use of random numbers and probability to solve complex problems based on trial and error. With the help of statistical theories , MC models are generally concerned with large numbers of numerical experiments using uncorrelated random numbers instead of deterministic algorithms. The main idea of solving state function integrals by randomly sampling from the non-uniform distribution of numbers was given by [172].

In the field of grain growth simulation, MC method discrete computation domain for the same and regular patterns. Each grid in the simulation domain is assigned with an integer number representing different crystals. Those adjacent grids with the same grain orientation belong to a single crystal grain. Based on the minimization of system free energy, the randomly selected nodes will change their orientations and visualized as the grain growth behavior. One thing to notice is that: this kind of MC model is only suitable for the solid-state grain growth, for example, the recrystallization and second-phase precipitation [173-177]. The limitation of the MC method is obvious that the growth kinetics are not considered in the simulation.

To achieve the solidification microstructure simulation for MAM process, the KMC method is adapted to investigate microstructure developed at the melt pool bottom [119, 121, 122]. The microstructure developed by different process parameters is compared, e.g., the scanning speed influence on microstructure shown in Fig. 5. The average size of the columnar grains in the fusion zone and the equiaxed grains in the heat affected zone was investigated and compared quantitatively with experiments. This can be attributed to the computational efficiency of KMC method which can be lauched in experimentatlly accessible time and length scales providing practical simulation result [178]. Due to the epitaxial grain growth in MAM, the grain growth from the liquid to the solid phase is simply treated as inheriting information from the partially melted grains according to the maximum heat flow direction. In the deposit layers, grain growth is simulated by KMC models as the migration of grain boundaries caused by the MC time [179].

Corresponding authors.
E-mail addresses: yaoyao.zhao@mcgill.ca (Y.F. Zhao), bkdzxl@gmail.com (X. Zhou)

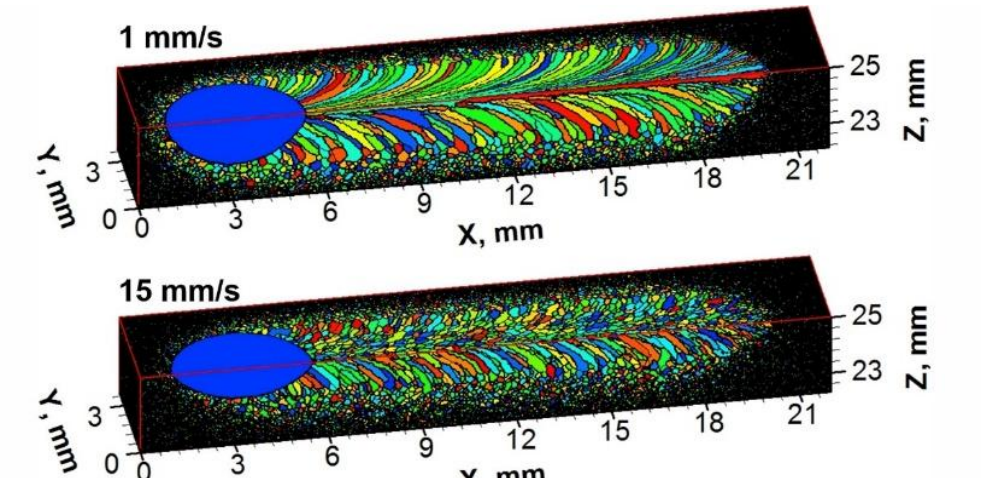

Fig 5*: KMC simulation of grain structures in a weld with different scanning speeds. [121]*

3.4 Needle-Network Method

In recent years, a novel dendritic needle network (DNN) method is introduced by [180] to unchain the scale limitation of PF method. This model represents the primary and high order branches of dendrites by thin needles which develop their own solute diffusion field and interact with each other. The growth dynamics of the needle crystals are derived from the Laplacian growth theory [181]. The tip velocity and radius are computed by considering two conditions: the standard solvability condition on the scale of dendrite tip and an additional flux balance condition on the outer scale of the dendritic network [182]. The target is to bridge the scale gap between PF and CA methods in the area of dendritic microstructure formation. Different from PF method, DNN does not focus on the tip scale solid-liquid interface but extend to grain scale with an acceptable loss of accuracy. On the other hand, this method reflects the competitive grain growth in a more natural way than CA method by considering both the history-dependent selection and the intergrain dendrite interactions. This model is implemented for both isothermal and directional solidification in 2D and validated by comparison with analytical solutions for equiaxed growth and PF simulations [182]. In their recently published works, a 3D version of needle-network was proposed and validated with an in-situ X-ray imaging of Al-Cu alloy solidification experiments [183]. A simplified version of needle network model has also been applied to study the epitaxial growth behavior of columnar grains and predict the texture in MAM process [184].

4. Discussion and Perspectives

Until now, most research works on the MAM microstructure simulation still focus on the deterministic methods based on experiments, for example, the effects of various process parameters on microstructure evolution in thermo-material models [17]. These models are sought by using the thermal history to predict microstructure evolution and the resulting temperature dependent material properties [46, 185, 186]. However, these deterministic methods are inadequate to describe the unique characteristics in MAM such as nucleation behavior, column grains, epitaxial growth, and anisotropy of material behaviors.

The reviewed solidification microstructure simulation methods all have their merits as well as the essential defects when applied in MAM. CA is currently the most suitable one among the reviewed methods for the solidification microstructure simulation in MAM with a relatively lower computational cost than PF, and a more solid physical basis compared to KMC. It has

Corresponding authors.
E-mail addresses: yaoyao.zhao@mcgill.ca (Y.F. Zhao), bkdzxl@gmail.com (X. Zhou)

recently been adapted as a module in commercial software (Ansys), which will accelerate its application development significantly. To describe the grain growth behavior, CA models are established based on the physics of dendrite tip kinetic to guarantee the simulation accuracy. On the other hand, CA method requires relatively low computation power, and the simulation can be applied into macroscale where it has more practical significances. PF method is firmly based on physical models and it is capable of providing a high reproduction of reality. It is also capable of describing the subgrain features like high order dendrites, micro-segregation, solid phase transformation and so on. However, PF models inherit minimal time and length scales from physical theories. The time steps of PF models are usually in the magnitude of microsecond or nondimensional number which must be small enough to stable the simulation result. Attaining a PF simulation even on micrometer-level requires massive computer power. A large amount of computation needed in the PF models makes it only feasible on supercomputers, therefore becomes an obstacle in the application. In order to simulate the grain competition during solidification, CA and PF methods have different strategies to endow the crystallographic structure of the grains considering their symmetry and preferential growth direction. KMC method has the advantage to efficiently simulate the migration of grain boundaries that occur in the solid state, but the crystallographic structures are not considered in most reviewed works, so its physical basis is not solid. It is also interesting to notice that the three methods start from different philosophical thoughts and methodologies but are applied to simulate the same objective in the case of MAM: CA method investigates the relationship between the part and the whole, it believes the physical state of the system is an aggregation of local state change; PF method attempts to describe the state of system by field parameters continuously, so it can avoid the difficulties lead by the sharp interface; for MC method, it uses a large number of sampling to approximate the truth, step by step. Even though there are significant differences among the three methods, they are all developed rapidly, especially in the field of microstructure simulation for MAM over the past decade.

MAM fabricated parts are composed of a large number of welds, the microstructure in a single weld bead will finally decide the initial microstructure of the MAM fabricated part at a specific position. Literature has already shown the importance of melt pool geometry to the final solidification microstructure in welding. It is very important to note that: the melt pool geometry is crucial for the resultant microstructure in MAM processes, and an accurate melt pool geometry is the prerequisite of an accurate microstructure simulation result. Solidification microstructure simulation for MAM must take proper consideration of melt pool geometry in terms of G&R and the boundary conditions established for each time step of the simulation. Melt pool geometry at the melt pool bottom is a curved surface to distinguish the solid and liquid phase. The thickness of this surface is the ambiguous area which is usually referred to as a mushy zone. The cooling condition along the melt pool bottom changes dramatically in terms of G&R, and in turn, influences the solidification microstructure developed subsequently. The melt pool geometry can be considered as a direct reflection of the cooling condition at the melt pool bottom, where solidification happens. Furthermore, the melt pool geometry follows the isothermal surface of the material, and the maximum thermal gradient direction can be captured from the geometric method. Then, the thermal gradient direction which means the maximum heat flux direction should be compared with the preferential growth direction of the crystal to reflect the competitive grain growth behavior accurately. Qualified CA and KMC work in MAM

Corresponding authors.
E-mail addresses: yaoyao.zhao@mcgill.ca (Y.F. Zhao), bkdzxl@gmail.com (X. Zhou)

microstructure simulation always consider the melt pool geometry explicitly or implicitly. However, it is still a problem for PF models as these models calculate hundreds of millions of cells/time steps over millions of time steps to place out the physics of the process long enough to be relevant. That is the reason why the PF models are mostly operated under the "frozen temperature approximation" not a field form of temperature representing the melt pool.

The melt pool geometry can also be used to bridge the scale gap. It can validate the simulation result in macro level and provide the boundary condition for the meso and micro level simulation. Some of the reviewed works used the melt pool simulation result directly as a boundary condition for solidification microstructure simulation. However, it usually leads to a more significant deviation when another simulation result is used as an input. Thus, the accuracy of these microstructure simulations is reduced as they do not have appropriate boundary conditions. Currently, highly developed techniques like CMOS camera [187, 188] and synchrotron X-ray [189, 190] can provide transient melt pool geometry with relatively high accuracy. These melt pool geometry reconstructions can be used as experimental validation for simulations and improve the accuracy.

The nucleation rule for the solidification microstructure simulation in MAM is still an open question in the literature. The assumption of epitaxial grain growth with no nucleation can only be applied to a small number of extreme cases in MAM. For powder bed, external factors (e.g., impurity, cracks, and unmelt metal powders) leave more opportunities for the nucleation in each weld and cannot be neglected. The contour of the melt pool will always bring new nucleation positions for solidification at the melt pool bottom. On the other hand, the grains in the DED process are typically considered to develop from the substrate, and the grains will stop growing at the contour without any new nucleation. This is close to the observed fact that the grains are able to develop extremely big and go through multiple layers, e.g., DED processed Ti-6Al-4V. Thus, in the case of the solidification microstructure simulations under "no nucleation assumption", it is more reasonable to establish the boundary condition of crystallographic orientation by experimental results (e.g., EBSD) instead of a random orientation assumption at the substrate.

Competitive grain growth is the subsequent step following nucleation. When the research area of the melt pool bottom is divided into very small length scale, the cooling condition can be considered as constant within a small timestep. The competitive grain growth of bi-crystal simulations is carried out under different methods and criterions where significant deviation on resultant grain boundary orientations are observed [191]. This is caused by the different assumptions and emphasis in different simulation methods: CA methods consider the problem on the kinetics aspect which links the dendrite tip growth rate with the supercooling; while PF method is derived on the thermodynamic aspects to represent the pattern change along with the free energy minimization. Unfortunately, this deviation on grain boundary orientations will become even larger when these models are applied to a more complicated problem. For example, the MAM microstructure simulation includes multiple crystals and a complicate cooling condition. A reasonable way to improve the microstructure simulation accuracy is the proper

Corresponding authors.
E-mail addresses: yaoyao.zhao@mcgill.ca (Y.F. Zhao), bkdzxl@gmail.com (X. Zhou)

model validation as well as the database establishment for each recognized phenomenon during the physical process.

The rapid solidification phenomenon makes the solidification microstructure simulation in MAM more difficult, especially the highly non-equilibrium phase transformation and the solute trapping effect in alloy systems. In CA method, the dendrite tip growth kinetics typically assume local equilibrium which is not valid under rapid cooling conditions. Another problem for CA models is that they typically use one layer of cells to represent the interface between liquid and solid with a solid fraction from zero to one [192], so it is difficult to naturally represent the solute trapping phenomenon. Also, as a rule of thumb, the cell size should be at least ten times smaller than the morphological features it captures. This methodology provides CA method a high computational efficiency, however, limits its smallest morphological length scale to depict finer microstructures (e.g. higher order branches) compared to the interface thickness. PF method is very quantitative in its description of solid-liquid interface kinetics. Recently, a work [68] introduced a strategy to quantitively map the thin interface behavior of an ideal dilute binary alloy PF model on to the continuous growth model. This strategy can be implemented in different phase field models, which will address this problem to a fair degree.

Simulation models for solid-state phase transformation is the indispensable part for the mechanical property prediction in MAM. It can be combined with the solidification microstructure simulation result then input into a failure model. These simulation efforts attempt to use the local history data (e.g. the thermal cycles profile in MAM) to predict the material dependent microstructural evolution including phase fraction and morphology [46, 193-198]. Recently, the density type simulation methods have been generally used for predicting microstructural evolution during solid-state phase transformations in MAM, especially for large-scale thermal/mechanical/metallurgical coupled problems. The phase fractions of diffusional and diffusionless phase transformation products and dependent properties could be effectively predicted using these methods if they are calibrated, accurately [199].

Model validation is essential for all kinds of simulation works. For the solidification microstructure simulation in MAM, however, the solid-state transformation, secondary or higher order branches merging, and the migration of grain boundaries brings great difficulties to recognize the original state and pattern of the solidification microstructure. Even though the reconstructed EBSD results provide accurate information in terms of crystallographic orientation and texture, they are only able to show the obscured grain geometry with no high order branch. Also, the grain geometry recognized by EBSD and the microscopes is usually operated at room temperature when the migration of grain boundaries has already occurred after the thermal cycles of MAM.

5. Conclusions

Developing a robust and accurate simulation model on a long scale to describe the grain growth behavior in a moving melt pool is still a challenge for MAM solidification microstructure simulation. An overview of all the microstructure simulation methods indicates that it is indeed important to develop an integrated and generalized model for MAM process, as a function of melt pool geometry and resultant microstructure. The paper further explains the sequential

Corresponding authors.
E-mail addresses: yaoyao.zhao@mcgill.ca (Y.F. Zhao), bkdzxl@gmail.com (X. Zhou)

dependency of each physical process during the solidification of MAM that is still open questions in the literature. To achieve an accurate simulation, database establishment between the recognized phenomena is the ideal method to fill these gaps by now. It is also important to know that: making a model with all the expected outcome does not lead to novel insights. As for the microstructure simulations in MAM, it is better to develop models carrying fundamental rules or model components from which more complex grain structure and texture can develop on its own. Otherwise, the simulation models are not predictive and are just pictures without new understanding.

Acknowledgment
This research was supported by the Natural Sciences and Engineering Research Council of Canada (NSERC) Collaborative Research and Development Grant CRDPJ 479630-15. The lead author also received partial funding from the NSERC Collaborative Research, Training Experience (CREATE) Program Grant 449343, and the National Key Research and Development Program of China (Grant No. 2018YFB0703400). The author would also like to thank McGill Engineering Doctoral Award (MEDA) grant and China Scholarship Council (201706460027).

Reference
[1] M. Taufik, P.K. Jain, Role of build orientation in layered manufacturing: a review, International Journal of Manufacturing Technology and Management 27(1-3) (2013) 47-73.
[2] M. Kumke, H. Watschke, P. Hartogh, A.K. Bavendiek, T. Vietor, Methods and tools for identifying and leveraging additive manufacturing design potentials, International Journal on Interactive Design and Manufacturing (IJIDeM) 12(2) (2018) 481-493.
[3] J.M. Wilson, C. Piya, Y.C. Shin, F. Zhao, K. Ramani, Remanufacturing of turbine blades by laser direct deposition with its energy and environmental impact analysis, Journal of Cleaner Production 80 (2014) 170-178.
[4] B. Dutta, F.H.S. Froes, The additive manufacturing (AM) of titanium alloys, Titanium powder metallurgy, Elsevier2015, pp. 447-468.
[5] D. Greitemeier, C. Dalle Donne, A. Schoberth, M. Jürgens, J. Eufinger, T. Melz, Uncertainty of Additive Manufactured Ti-6Al-4V: Chemistry, Microstructure and Mechanical Properties, Applied Mechanics and Materials 807 (2015) 169-180.
[6] M. Markl, C. Körner, Multiscale Modeling of Powder Bed–Based Additive Manufacturing, Annual Review of Materials Research 46(1) (2016) 93-123.
[7] W.E. Frazier, Metal Additive Manufacturing: A Review, J. Mater. Eng. Perform. 23(6) (2014) 1917-1928.
[8] V.V. Semak, Melt pool dynamics during laser welding, J. Phys. D: Appl. Phys. 28 (1995) 2443.
[9] F. Karimzadeh, A. Ebnonnasir, A. Foroughi, Artificial neural network modeling for evaluating of epitaxial growth of Ti6Al4V weldment, Materials Science and Engineering: A 432(1-2) (2006) 184-190.
[10] S. David, S. Babu, J. Vitek, Welding: Solidification and microstructure, JOM 55(6) (2003) 14-20.
[11] W.J. Sames, F.A. List, S. Pannala, R.R. Dehoff, S.S. Babu, The metallurgy and processing science of metal additive manufacturing, Int. Mater. Rev. 61(5) (2016) 315-360.
[12] N. Raghavan, R. Dehoff, S. Pannala, S. Simunovic, M. Kirka, J. Turner, N. Carlson, S.S. Babu, Numerical modeling of heat-transfer and the influence of process parameters on tailoring the grain morphology of IN718 in electron beam additive manufacturing, Acta Mater. 112 (2016) 303-314.
[13] J.J. Lin, Y.H. Lv, Y.X. Liu, B.S. Xu, Z. Sun, Z.G. Li, Y.X. Wu, Microstructural evolution and mechanical properties of Ti-6Al-4V wall deposited by pulsed plasma arc additive manufacturing, Materials & Design 102 (2016) 30-40.

Corresponding authors.
E-mail addresses: yaoyao.zhao@mcgill.ca (Y.F. Zhao), bkdzxl@gmail.com (X. Zhou)

[14] D. Herzog, V. Seyda, E. Wycisk, C. Emmelmann, Additive manufacturing of metals, Acta Mater. 117 (2016) 371-392.
[15] F. Wang, S. Williams, P. Colegrove, A.A. Antonysamy, Microstructure and Mechanical Properties of Wire and Arc Additive Manufactured Ti-6Al-4V, MMTA 44(2) (2012) 968-977.
[16] F. Wang, S. Williams, M. Rush, Morphology investigation on direct current pulsed gas tungsten arc welded additive layer manufactured Ti6Al4V alloy, The International Journal of Advanced Manufacturing Technology 57(5-8) (2011) 597-603.
[17] P. Kobryn, S. Semiatin, The laser additive manufacture of Ti-6Al-4V, JOM 53(9) (2001) 40-42.
[18] L. Thijs, F. Verhaeghe, T. Craeghs, J. Van Humbeeck, J.P. Kruth, A study of the microstructural evolution during selective laser melting of Ti–6Al–4V, Acta Mater. 58(9) (2010) 3303-3312.
[19] S. Bontha, N.W. Klingbeil, P.A. Kobryn, H.L. Fraser, Thermal process maps for predicting solidification microstructure in laser fabrication of thin-wall structures, J. Mater. Process. Technol. 178(1-3) (2006) 135-142.
[20] M. Gäumann, S. Henry, F. Cleton, J.-D. Wagniere, W. Kurz, Epitaxial laser metal forming: analysis of microstructure formation, Materials Science and Engineering: A 271(1-2) (1999) 232-241.
[21] T. Wang, Y.Y. Zhu, S.Q. Zhang, H.B. Tang, H.M. Wang, Grain morphology evolution behavior of titanium alloy components during laser melting deposition additive manufacturing, J. Alloys Compd. 632 (2015) 505-513.
[22] B. Cai, J. Wang, A. Kao, K. Pericleous, A.B. Phillion, R.C. Atwood, P.D. Lee, 4D synchrotron X-ray tomographic quantification of the transition from cellular to dendrite growth during directional solidification, Acta Mater. 117 (2016) 160-169.
[23] G.C. Obasi, S. Birosca, J. Quinta da Fonseca, M. Preuss, Effect of β grain growth on variant selection and texture memory effect during $\alpha \rightarrow \beta \rightarrow \alpha$ phase transformation in Ti‑6 Al‑4 V, Acta Mater. 60(3) (2012) 1048-1058.
[24] A.A. Antonysamy, P.B. Prangnell, J. Meyer, Effect of Wall Thickness Transitions on Texture and Grain Structure in Additive Layer Manufacture (ALM) of Ti-6Al-4V, Mater. Sci. Forum 706-709 (2012) 205-210.
[25] S.S. Al-Bermani, M.L. Blackmore, W. Zhang, I. Todd, The Origin of Microstructural Diversity, Texture, and Mechanical Properties in Electron Beam Melted Ti-6Al-4V, MMTA 41(13) (2010) 3422-3434.
[26] L. Thijs, M.L. Montero Sistiaga, R. Wauthle, Q. Xie, J.-P. Kruth, J. Van Humbeeck, Strong morphological and crystallographic texture and resulting yield strength anisotropy in selective laser melted tantalum, Acta Mater. 61(12) (2013) 4657-4668.
[27] A.A. Antonysamy, J. Meyer, P.B. Prangnell, Effect of build geometry on the β-grain structure and texture in additive manufacture of Ti6Al4V by selective electron beam melting, Mater. Charact. 84 (2013) 153-168.
[28] M. Glavicic, P. Kobryn, T. Bieler, S. Semiatin, A method to determine the orientation of the high-temperature beta phase from measured EBSD data for the low-temperature alpha phase in Ti-6Al-4V, Materials Science and Engineering: A 346(1-2) (2003) 50-59.
[29] C. Cayron, B. Artaud, L. Briottet, Reconstruction of parent grains from EBSD data, Mater. Charact. 57(4-5) (2006) 386-401.
[30] C. Cayron, Groupoid of orientational variants, Acta Crystallogr. Sect. A: Found. Crystallogr. 62(1) (2006) 21-40.
[31] A. Basak, S. Das, Epitaxy and Microstructure Evolution in Metal Additive Manufacturing, Annual Review of Materials Research 46(1) (2016) 125-149.
[32] B. Ellyson, N. Chekir, M. Brochu, M. Brochu, Characterization of bending vibration fatigue of WBD fabricated Ti-6Al-4V, Int. J. Fatigue 101 (2017) 36-44.
[33] F. Wang, J. Mei, X. Wu, Microstructure study of direct laser fabricated Ti alloys using powder and wire, Appl. Surf. Sci. 253(3) (2006) 1424-1430.

Corresponding authors.
E-mail addresses: yaoyao.zhao@mcgill.ca (Y.F. Zhao), bkdzxl@gmail.com (X. Zhou)

[34] B. Vrancken, L. Thijs, J.-P. Kruth, J. Van Humbeeck, Heat treatment of Ti6Al4V produced by Selective Laser Melting: Microstructure and mechanical properties, J. Alloys Compd. 541 (2012) 177-185.
[35] P. Kontis, E. Chauvet, Z. Peng, J. He, A.K.d. Silva, D. Raabe, C. Tassin, J.-J. Blandin, S. Abed, R. Dendievel, Atomic-scale grain boundary engineering to overcome hot-cracking in additively-manufactured superalloys, Available at SSRN 3391502 (2019).
[36] B.E. Carroll, T.A. Palmer, A.M. Beese, Anisotropic tensile behavior of Ti–6Al–4V components fabricated with directed energy deposition additive manufacturing, Acta Mater. 87 (2015) 309-320.
[37] S. Kumar, W.A. Curtin, Crack interaction with microstructure, Mater. Today 10(9) (2007) 34-44.
[38] Y. Kok, X.P. Tan, P. Wang, M.L.S. Nai, N.H. Loh, E. Liu, S.B. Tor, Anisotropy and heterogeneity of microstructure and mechanical properties in metal additive manufacturing: A critical review, Materials & Design 139 (2018) 565-586.
[39] J. Wang, X. Lin, J. Wang, H. Yang, Y. Zhou, C. Wang, Q. Li, W. Huang, Grain morphology evolution and texture characterization of wire and arc additive manufactured Ti-6Al-4V, J. Alloys Compd. 768 (2018) 97-113.
[40] P. Liu, Z. Wang, Y. Xiao, M.F. Horstemeyer, X. Cui, L. Chen, Insight into the mechanisms of columnar to equiaxed grain transition during metallic additive manufacturing, Additive Manufacturing 26 (2019) 22-29.
[41] J.A. Dantzig, M. Rappaz, Solidification, EPFL press2009.
[42] S. Liu, Y.C. Shin, Additive manufacturing of Ti6Al4V alloy: A review, Materials & Design 164 (2019) 107552.
[43] K.A. Lee, Y.K. Kim, J.H. Yu, S.H. Park, M.C. Kim, Effect of Heat Treatment on Microstructure and Impact Toughness of Ti-6Al-4V Manufactured by Selective Laser Melting Process, Archives of Metallurgy and Materials 62(2) (2017) 1341-1346.
[44] A.M. Beese, B.E. Carroll, Review of Mechanical Properties of Ti-6Al-4V Made by Laser-Based Additive Manufacturing Using Powder Feedstock, JOM 68(3) (2015) 724-734.
[45] T. Ahmed, H. Rack, Phase transformations during cooling in α+ β titanium alloys, Materials Science and Engineering: A 243(1) (1998) 206-211.
[46] S.M.K.a.S.L. KAMPE, Microstructural Evolution in Laser-Deposited Multilayer Ti-6Al-4V Builds, MMTA 35(6) (2004) 1861-1867.
[47] G. Lütjering, Influence of processing on microstructure and mechanical properties of (α+ β) titanium alloys, Materials Science and Engineering: A 243(1-2) (1998) 32-45.
[48] P. Haasen, The early stages of the decomposition of alloys, Metall. Trans. A 16(7) (1985) 1173-1184.
[49] G.C. Sosso, J. Chen, S.J. Cox, M. Fitzner, P. Pedevilla, A. Zen, A. Michaelides, Crystal Nucleation in Liquids: Open Questions and Future Challenges in Molecular Dynamics Simulations, Chem. Rev. 116(12) (2016) 7078-116.
[50] Y. Shibuta, S. Sakane, E. Miyoshi, S. Okita, T. Takaki, M. Ohno, Heterogeneity in homogeneous nucleation from billion-atom molecular dynamics simulation of solidification of pure metal, Nature Communications 8(1) (2017) 10.
[51] S. David, S. Babu, Microstructure modeling in weld metal, Oak Ridge National Lab., 1995.
[52] S.A. David, J.M. Vitek, M. Rappaz, L.A. Boatner, Microstructure of stainless steel single-crystal electron beam welds, Metall. Trans. A 21(6) (1990) 1753-1766.
[53] T. Zacharia, J. Vitek, J. Goldak, T. DebRoy, M. Rappaz, H. Bhadeshia, Modeling of fundamental phenomena in welds, Modell. Simul. Mater. Sci. Eng. 3(2) (1995) 265.
[54] T. DebRoy, S. David, Physical processes in fusion welding, RvMP 67(1) (1995) 85.
[55] S. David, J. Vitek, Correlation between solidification parameters and weld microstructures, Int. Mater. Rev. 34(1) (1989) 213-245.

Corresponding authors.
E-mail addresses: yaoyao.zhao@mcgill.ca (Y.F. Zhao), bkdzxl@gmail.com (X. Zhou)

[56] M. Griffith, M. Schlienger, L. Harwell, M. Oliver, M. Baldwin, M. Ensz, M. Essien, J. Brooks, C. Robino, e.J. Smugeresky, Understanding thermal behavior in the LENS process, Materials & Design 20(2-3) (1999) 107-113.
[57] M. Gouge, P. Michaleris, Thermo-mechanical Modeling of Additive Manufacturing, Butterworth-Heinemann2017.
[58] D.M. Keicher, J.E. Smugeresky, The laser forming of metallic components using particulate materials, JOM 49(5) (1997) 51-54.
[59] L.E. Murr, S.M. Gaytan, D.A. Ramirez, E. Martinez, J. Hernandez, K.N. Amato, P.W. Shindo, F.R. Medina, R.B. Wicker, Metal Fabrication by Additive Manufacturing Using Laser and Electron Beam Melting Technologies, Journal of Materials Science & Technology 28(1) (2012) 1-14.
[60] Y.C. Shin, N. Bailey, C. Katinas, W. Tan, Predictive modeling capabilities from incident powder and laser to mechanical properties for laser directed energy deposition, CompM 61(5) (2018) 617-636.
[61] J.C. Heigel, P. Michaleris, E.W. Reutzel, Thermo-mechanical model development and validation of directed energy deposition additive manufacturing of Ti–6Al–4V, Additive Manufacturing 5 (2015) 9-19.
[62] A. Zinoviev, O. Zinovieva, V. Ploshikhin, V. Romanova, R. Balokhonov, Evolution of grain structure during laser additive manufacturing. Simulation by a cellular automata method, Materials & Design 106 (2016) 321-329.
[63] J. Zhang, F. Liou, W. Seufzer, K. Taminger, A coupled finite element cellular automaton model to predict thermal history and grain morphology of Ti-6Al-4V during direct metal deposition (DMD), Additive Manufacturing 11 (2016) 32-39.
[64] A. Rai, M. Markl, C. Körner, A coupled Cellular Automaton–Lattice Boltzmann model for grain structure simulation during additive manufacturing, Computational Materials Science 124 (2016) 37-48.
[65] S.M. Thompson, L. Bian, N. Shamsaei, A. Yadollahi, An overview of Direct Laser Deposition for additive manufacturing; Part I: Transport phenomena, modeling and diagnostics, Additive Manufacturing 8 (2015) 36-62.
[66] M.J. Aziz, T. Kaplan, Continuous growth model for interface motion during alloy solidification, Acta Metall. 36(8) (1988) 2335-2347.
[67] N. Ahmad, A. Wheeler, W.J. Boettinger, G.B. McFadden, Solute trapping and solute drag in a phase-field model of rapid solidification, PhRvE 58(3) (1998) 3436.
[68] T. Pinomaa, N. Provatas, Quantitative phase field modeling of solute trapping and continuous growth kinetics in quasi-rapid solidification, Acta Mater. 168 (2019) 167-177.
[69] D. Danilov, B. Nestler, Phase-field modelling of solute trapping during rapid solidification of a Si–As alloy, Acta Mater. 54(18) (2006) 4659-4664.
[70] P. Galenko, E. Abramova, D. Jou, D. Danilov, V. Lebedev, D.M. Herlach, Solute trapping in rapid solidification of a binary dilute system: a phase-field study, PhRvE 84(4) (2011) 041143.
[71] X. Li, W. Tan, Numerical investigation of effects of nucleation mechanisms on grain structure in metal additive manufacturing, Computational Materials Science 153 (2018) 159-169.
[72] J.A. Koepf, M.R. Gotterbarm, M. Markl, C. Körner, 3D multi-layer grain structure simulation of powder bed fusion additive manufacturing, Acta Mater. 152 (2018) 119-126.
[73] O. Zinovieva, A. Zinoviev, V. Ploshikhin, Three-dimensional modeling of the microstructure evolution during metal additive manufacturing, Computational Materials Science 141 (2018) 207-220.
[74] J. Koepf, D. Soldner, M. Ramsperger, J. Mergheim, M. Markl, C. Körner, Numerical microstructure prediction by a coupled finite element cellular automaton model for selective electron beam melting, Computational Materials Science 162 (2019) 148-155.
[75] S. Chen, G. Guillemot, C.-A. Gandin, Three-dimensional cellular automaton-finite element modeling of solidification grain structures for arc-welding processes, Acta Mater. 115 (2016) 448-467.

Corresponding authors.
E-mail addresses: yaoyao.zhao@mcgill.ca (Y.F. Zhao), bkdzxl@gmail.com (X. Zhou)

[76] R. Shi, S. Khairallah, T.W. Heo, M. Rolchigo, J.T. McKeown, M.J. Matthews, Integrated Simulation Framework for Additively Manufactured Ti-6Al-4V: Melt Pool Dynamics, Microstructure, Solid-State Phase Transformation, and Microelastic Response, JOM (2019) 1-16.
[77] A.R. Dezfoli, W.S. Hwang, W.C. Huang, T.W. Tsai, Determination and controlling of grain structure of metals after laser incidence: Theoretical approach, Scientific Reports 7 (2017) 41527.
[78] C. Gu, Y. Wei, X. Zhan, Y. Li, A three-dimensional cellular automaton model of dendrite growth with stochastic orientation during the solidification in the molten pool of binary alloy, Sci. Technol. Weld. Joining 22(1) (2016) 47-58.
[79] W. Yan, Y. Lian, C. Yu, O.L. Kafka, Z. Liu, W.K. Liu, G.J. Wagner, An integrated process–structure–property modeling framework for additive manufacturing, CMAME 339 (2018) 184-204.
[80] M. Rolchigo, R. LeSar, Application of alloy solidification theory to cellular automata modeling of near-rapid constrained solidification, Computational Materials Science 163 (2019) 148-161.
[81] A. Rai, H. Helmer, C. Körner, Simulation of grain structure evolution during powder bed based additive manufacturing, Additive Manufacturing 13 (2017) 124-134.
[82] O. Lopez-Botello, U. Martinez-Hernandez, J. Ramírez, C. Pinna, K. Mumtaz, Two-dimensional simulation of grain structure growth within selective laser melted AA-2024, Materials & Design 113 (2017) 369-376.
[83] H. Yin, S.D. Felicelli, Dendrite growth simulation during solidification in the LENS process, Acta Mater. 58(4) (2010) 1455-1465.
[84] Z.J. Wang, S. Luo, H.W. Song, W.D. Deng, W.Y. Li, Simulation of Microstructure during Laser Rapid Forming Solidification Based on Cellular Automaton, Mathematical Problems in Engineering 2014 (2014) 1-9.
[85] H. Yin, S.D. Felicelli, L. Wang, Simulation of a dendritic microstructure with the lattice Boltzmann and cellular automaton methods, Acta Mater. 59(8) (2011) 3124-3136.
[86] T. Carozzani, C.-A. Gandin, H. Digonnet, M. Bellet, K. Zaidat, Y. Fautrelle, Direct Simulation of a Solidification Benchmark Experiment, MMTA 44(2) (2012) 873-887.
[87] C.-A. Gandin, J.-L. Desbiolles, M. Rappaz, P. Thevoz, A three-dimensional cellular automation-finite element model for the prediction of solidification grain structures, MMTA 30(12) (1999) 3153-3165.
[88] T. Carozzani, H. Digonnet, C.-A. Gandin, 3D CAFE modeling of grain structures: application to primary dendritic and secondary eutectic solidification, Modell. Simul. Mater. Sci. Eng. 20(1) (2011) 015010.
[89] C.A. Gandin, T. Carozzani, H. Digonnet, S. Chen, G. Guillemot, Direct Modeling of Structures and Segregations Up to Industrial Casting Scales, JOM 65(9) (2013) 1122-1130.
[90] W. Wang, P.D. Lee, M. Mclean, A model of solidification microstructures in nickel-based superalloys: predicting primary dendrite spacing selection, Acta Mater. 51(10) (2003) 2971-2987.
[91] M. Rappaz, C.-A. Gandin, Probabilistic modelling of microstructure formation in solidification processes, AcM&M 41(2) (1993) 345-360.
[92] L. Nastac, Numerical modeling of solidification morphologies and segregation patterns in cast dendritic alloys, Acta Mater. 47(17) (1999) 4253-4262.
[93] X. Zhan, Y. Wei, Z. Dong, Cellular automaton simulation of grain growth with different orientation angles during solidification process, J. Mater. Process. Technol. 208(1-3) (2008) 1-8.
[94] B. Radhakrishnan, S.B. Gorti, J.A. Turner, R. Acharya, J.A. Sharon, A. Staroselsky, T. El-Wardany, Phase Field Simulations of Microstructure Evolution in IN718 using a Surrogate Ni–Fe–Nb Alloy during Laser Powder Bed Fusion, Metals 9(1) (2019) 14.
[95] S. Ghosh, K. McReynolds, J.E. Guyer, D. Banerjee, Simulation of temperature, stress and microstructure fields during laser deposition of Ti–6Al–4V, Modell. Simul. Mater. Sci. Eng. 26(7) (2018) 075005.

Corresponding authors.
E-mail addresses: yaoyao.zhao@mcgill.ca (Y.F. Zhao), bkdzxl@gmail.com (X. Zhou)

[96] L.X. Lu, N. Sridhar, Y.W. Zhang, Phase field simulation of powder bed-based additive manufacturing, Acta Mater. 144 (2018) 801-809.
[97] R. Acharya, J.A. Sharon, A. Staroselsky, Prediction of microstructure in laser powder bed fusion process, Acta Mater. 124 (2017) 360-371.
[98] T. Keller, G. Lindwall, S. Ghosh, L. Ma, B.M. Lane, F. Zhang, U.R. Kattner, E.A. Lass, J.C. Heigel, Y. Idell, Application of finite element, phase-field, and CALPHAD-based methods to additive manufacturing of Ni-based superalloys, Acta Mater. 139 (2017) 244-253.
[99] D. Liu, Y. Wang, Mesoscale Multi-Physics Simulation of Solidification in Selective Laser Melting Process Using a Phase Field and Thermal Lattice Boltzmann Model, ASME 2017 International Design Engineering Technical Conferences and Computers and Information in Engineering Conference, American Society of Mechanical Engineers, 2017, pp. V001T02A027-V001T02A027.
[100] X. Wang, K. Chou, Microstructure simulations of Inconel 718 during selective laser melting using a phase field model, The International Journal of Advanced Manufacturing Technology 100(9-12) (2019) 2147-2162.
[101] L. Wu, J. Zhang, Phase Field Simulation of Dendritic Solidification of Ti-6Al-4V During Additive Manufacturing Process, JOM 70(10) (2018) 2392-2399.
[102] J. Kundin, A. Ramazani, U. Prahl, C. Haase, Microstructure Evolution of Binary and Multicomponent Manganese Steels During Selective Laser Melting: Phase-Field Modeling and Experimental Validation, MMTA 50(4) (2019) 2022-2040.
[103] N. Xue, Y. Ren, X. Ren, N. Ren, Q. Lin, Q. Wang, K. Qin, Phase filed simulation of dendritic growth of copper films irradiated by ultrashort laser pulses, Computational Materials Science 148 (2018) 60-68.
[104] T. Takaki, T. Shimokawabe, M. Ohno, A. Yamanaka, T. Aoki, Unexpected selection of growing dendrites by very-large-scale phase-field simulation, J. Cryst. Growth 382 (2013) 21-25.
[105] C. Yang, Q. Xu, B. Liu, GPU-accelerated three-dimensional phase-field simulation of dendrite growth in a nickel-based superalloy, Computational Materials Science 136 (2017) 133-143.
[106] P. Steinmetz, J. Hötzer, M. Kellner, A. Genau, B. Nestler, Study of pattern selection in 3D phase-field simulations during the directional solidification of ternary eutectic Al-Ag-Cu, Computational Materials Science 148 (2018) 131-140.
[107] T. Gong, Y. Chen, Y. Cao, X. Kang, D. Li, Fast simulations of a large number of crystals growth in centimeter-scale during alloy solidification via nonlinearly preconditioned quantitative phase-field formula, Computational Materials Science 147 (2018) 338-352.
[108] N. Bergeon, D. Tourret, L. Chen, J.-M. Debierre, R. Guérin, A. Ramirez, B. Billia, A. Karma, R. Trivedi, Spatiotemporal dynamics of oscillatory cellular patterns in three-dimensional directional solidification, Phys. Rev. Lett. 110(22) (2013) 226102.
[109] A. Karma, D. Tourret, Atomistic to continuum modeling of solidification microstructures, Curr. Opin. Solid State Mater. Sci. 20(1) (2016) 25-36.
[110] A.J. Clarke, D. Tourret, Y. Song, S.D. Imhoff, P.J. Gibbs, J.W. Gibbs, K. Fezzaa, A. Karma, Microstructure selection in thin-sample directional solidification of an Al-Cu alloy: In situ X-ray imaging and phase-field simulations, Acta Mater. 129 (2017) 203-216.
[111] R.-w. Geng, J. Du, Z.-y. Wei, G.-x. Zhao, Simulation of microstructure evolution in fused-coating additive manufacturing based on phase field approach, China Foundry 14(5) (2017) 346-352.
[112] D. Tourret, A. Karma, Growth competition of columnar dendritic grains: A phase-field study, Acta Mater. 82 (2015) 64-83.
[113] T. Takaki, M. Ohno, T. Shimokawabe, T. Aoki, Two-dimensional phase-field simulations of dendrite competitive growth during the directional solidification of a binary alloy bicrystal, Acta Mater. 81 (2014) 272-283.

Corresponding authors.
E-mail addresses: yaoyao.zhao@mcgill.ca (Y.F. Zhao), bkdzxl@gmail.com (X. Zhou)

[114] H. Humadi, N. Ofori-Opoku, N. Provatas, J.J. Hoyt, Atomistic Modeling of Solidification Phenomena Using the Phase-Field-Crystal Model, JOM 65(9) (2013) 1103-1110.
[115] W.J. Boettinger, J.A. Warren, C. Beckermann, A. Karma, Phase-Field Simulation of Solidification, Annual Review of Materials Research 32(1) (2002) 163-194.
[116] S.G. Kim, W.T. Kim, Phase-field modeling of rapid solidification, Materials Science and Engineering: A 304 (2001) 281-286.
[117] D. Tourret, Y. Song, A.J. Clarke, A. Karma, Grain growth competition during thin-sample directional solidification of dendritic microstructures: A phase-field study, Acta Mater. 122 (2017) 220-235.
[118] N. Warnken, D. Ma, A. Drevermann, R.C. Reed, S.G. Fries, I. Steinbach, Phase-field modelling of as-cast microstructure evolution in nickel-based superalloys, Acta Mater. 57(19) (2009) 5862-5875.
[119] H. Wei, G. Knapp, T. Mukherjee, T. DebRoy, Three-dimensional grain growth during multi-layer printing of a nickel-based alloy Inconel 718, Additive Manufacturing (2018).
[120] Z. Yang, S. Sista, J. Elmer, T. DebRoy, Three dimensional Monte Carlo simulation of grain growth during GTA welding of titanium, Acta Mater. 48(20) (2000) 4813-4825.
[121] H.L. Wei, J.W. Elmer, T. DebRoy, Three-dimensional modeling of grain structure evolution during welding of an aluminum alloy, Acta Mater. 126 (2017) 413-425.
[122] H. Wei, J. Elmer, T. DebRoy, Crystal growth during keyhole mode laser welding, Acta Mater. 133 (2017) 10-20.
[123] H.L. Wei, J. Mazumder, T. DebRoy, Evolution of solidification texture during additive manufacturing, Scientific Reports 5 (2015) 16446.
[124] H.L. Wei, J.W. Elmer, T. DebRoy, Origin of grain orientation during solidification of an aluminum alloy, Acta Mater. 115 (2016) 123-131.
[125] D. Raabe, Computational Materials Science, WILEY-VCH1998.
[126] S. Wolfram, Cellular automata as models of complexity, Nature 311(5985) (1984) 419.
[127] S. Wolfram, Computation theory of cellular automata, CMaPh 96(1) (1984) 15-57.
[128] Y. Zhuang, W. LI, H. Wang, S. Hong, H. Wang, A Bibliographic Review of Cellular Automaton Publications in the Last 50 Years, Journal of Cellular Automata 12(6) (2017) 475-492.
[129] L.O. Chua, L. Yang, Cellular neural networks: Applications, IEEE Transactions on circuits and systems 35(10) (1988) 1273-1290.
[130] D. Raabe, Cellular Automata in Materials Science with Particular Reference to Recrystallization Simulation, Annual Review of Materials Research 32(1) (2002) 53-76.
[131] D. Raabe, R.C. Becker, Coupling of a crystal plasticity finite-element model with a probabilistic cellular automaton for simulating primary static recrystallization in aluminium, Modell. Simul. Mater. Sci. Eng. 8(4) (2000) 445.
[132] D. Raabe, L. Hantcherli, 2D cellular automaton simulation of the recrystallization texture of an IF sheet steel under consideration of Zener pinning, Computational Materials Science 34(4) (2005) 299-313.
[133] D. Raabe, Mesoscale simulation of recrystallization textures and microstructures, Adv. Eng. Mater. 3(10) (2001) 745.
[134] D. Raabe, Introduction of a scalable three-dimensional cellular automaton with a probabilistic switching rule for the discrete mesoscale simulation of recrystallization phenomena, Philos. Mag. A 79(10) (1999) 2339-2358.
[135] M. Qian, Z.X. Guo, Cellular automata simulation of microstructural evolution during dynamic recrystallization of an HY-100 steel, Materials Science and Engineering: A 365(1-2) (2004) 180-185.
[136] T. Zhang, S. Lu, Y. Wu, G. Hai, Optimization of deformation parameters of dynamic recrystallization for 7055 aluminum alloy by cellular automaton, Transactions of Nonferrous Metals Society of China 27(6) (2017) 1327-1337.

Corresponding authors.
E-mail addresses: yaoyao.zhao@mcgill.ca (Y.F. Zhao), bkdzxl@gmail.com (X. Zhou)

[137] C. Gu, Y. Wei, F. Yu, X. Liu, L. She, Cellular Automaton Study of Hydrogen Porosity Evolution Coupled with Dendrite Growth During Solidification in the Molten Pool of Al-Cu Alloys, MMTA 48(9) (2017) 4314-4323.
[138] M. Picasso, C. Marsden, J. Wagniere, A. Frenk, M. Rappaz, A simple but realistic model for laser cladding, Metallurgical and Materials Transactions B 25(2) (1994) 281-291.
[139] C.-A. Gandin, M. Rappaz, R. Tintillier, 3-dimensional simulation of the grain formation in investment castings, MMTA 25(3) (1994) 629-635.
[140] C.-A. Gandin, M. Rappaz, A coupled finite element-cellular automaton model for the prediction of dendritic grain structures in solidification processes, AcM&M 42(7) (1994) 2233-2246.
[141] C.-A. Gandin, M. Rappaz, A 3D cellular automaton algorithm for the prediction of dendritic grain growth, Acta Mater. 45(5) (1997) 2187-2195.
[142] M. Rappaz, Modeling and characterization of grain structures and defects in solidification, Curr. Opin. Solid State Mater. Sci. 20(1) (2016) 37-45.
[143] L. Yuan, P.D. Lee, A new mechanism for freckle initiation based on microstructural level simulation, Acta Mater. 60(12) (2012) 4917-4926.
[144] J.Z. Yi, P.D. Lee, T.C. Lindley, T. Fukui, Statistical modeling of microstructure and defect population effects on the fatigue performance of cast A356-T6 automotive components, Materials Science and Engineering: A 432(1-2) (2006) 59-68.
[145] H.B. Dong, P.D. Lee, Simulation of the columnar-to-equiaxed transition in directionally solidified Al–Cu alloys, Acta Mater. 53(3) (2005) 659-668.
[146] N. D'souza, P. Jennings, X. Yang, P. Lee, M. McLean, H. Dong, Seeding of single-crystal superalloys—Role of constitutional undercooling and primary dendrite orientation on stray-grain nucleation and growth, Metallurgical and Materials Transactions B 36(5) (2005) 657-666.
[147] R.C. Atwood, P.D. Lee, Simulation of the three-dimensional morphology of solidification porosity in an aluminium–silicon alloy, Acta Mater. 51(18) (2003) 5447-5466.
[148] P. Lee, A. Chirazi, D. See, Modeling microporosity in aluminum–silicon alloys: a review, Journal of light metals 1(1) (2001) 15-30.
[149] A. Shterenlikht, L. Margetts, Three-dimensional cellular automata modelling of cleavage propagation across crystal boundaries in polycrystalline microstructures, Proceedings of the Royal Society A: Mathematical, Physical and Engineering Sciences 471(2177) (2015) 20150039-20150039.
[150] W. Kurz, B. Giovanola, R. Trivedi, Theory of microstructural development during rapid solidification, Acta Metall. 34(5) (1986) 823-830.
[151] D.C. Tsai, W.S. Hwang, A three dimensional cellular automaton model for the prediction of solidification morphologies of brass alloy by horizontal continuous casting and its experimental verification, Materials transactions 52(4) (2011) 787-794.
[152] J. Warren, Dendritic crystals: rule of thumb breaks down, Nature materials 5(8) (2006) 595.
[153] T. Haxhimali, A. Karma, F. Gonzales, M. Rappaz, Orientation selection in dendritic evolution, Nature materials 5(8) (2006) 660.
[154] I. Steinbach, Why Solidification? Why Phase-Field?, JOM 65(9) (2013) 1096-1102.
[155] L. Wang, N. Wang, N. Provatas, Liquid channel segregation and morphology and their relation with hot cracking susceptibility during columnar growth in binary alloys, Acta Mater. 126 (2017) 302-312.
[156] V. Fallah, A. Korinek, N. Ofori-Opoku, B. Raeisinia, M. Gallerneault, N. Provatas, S. Esmaeili, Atomic-scale pathway of early-stage precipitation in Al–Mg–Si alloys, Acta Mater. 82 (2015) 457-467.
[157] N. Provatas, J. Dantzig, B. Athreya, P. Chan, P. Stefanovic, N. Goldenfeld, K. Elder, Using the phase-field crystal method in the multi-scale modeling of microstructure evolution, JOM 59(7) (2007) 83-90.
[158] K. Ahmed, T. Allen, A. El-Azab, Phase field modeling for grain growth in porous solids, JMatS 51(3) (2015) 1261-1277.

Corresponding authors.
E-mail addresses: yaoyao.zhao@mcgill.ca (Y.F. Zhao), bkdzxl@gmail.com (X. Zhou)

[159] S. Hu, L. Chen, Solute segregation and coherent nucleation and growth near a dislocation—a phase-field model integrating defect and phase microstructures, Acta Mater. 49(3) (2001) 463-472.
[160] T.T. Nguyen, J. Yvonnet, Q.Z. Zhu, M. Bornert, C. Chateau, A phase field method to simulate crack nucleation and propagation in strongly heterogeneous materials from direct imaging of their microstructure, EnFM 139 (2015) 18-39.
[161] N. Provatas, K. Elder, Phase-field methods in materials science and engineering, John Wiley & Sons2011.
[162] G. Nash, M. Glicksman, Capillaritl-limited steadl-state dendritic grolth—I. Theoretical development, Acta Metall. 22(10) (1974) 1283-1290.
[163] J. Langer, H. Müller-Krumbhaar, Theory of dendritic growth—I. Elements of a stability analysis, Acta Metall. 26(11) (1978) 1681-1687.
[164] D.A. Kessler, J. Koplik, H. Levine, Pattern formation far from equilibrium: the free space dendritic crystal, Patterns, Defects and Microstructures in Nonequilibrium Systems, Springer1987, pp. 1-11.
[165] J.J. Xu, Interfacial Wave Theory of Pattern Formation in Solidification, Springer Series in Synergetics (Complexity) (2017) 16-21.
[166] J.W. Cahn, J.E. Hilliard, Spinodal decomposition: A reprise, Acta Metall. 19(2) (1971) 151-161.
[167] J.W. Cahn, J.E. Hilliard, Free energy of a nonuniform system. I. Interfacial free energy, The Journal of Chemical Physics 28(2) (1958) 258-267.
[168] L.P. Gor'kov, Microscopic derivation of the Ginzburg-Landau equations in the theory of superconductivity, Sov. Phys. JETP 9(6) (1959) 1364-1367.
[169] L.Q. Chen, Phase-field models for microstructure evolution, Annual review of materials research 32(1) (2002) 113-140.
[170] L. Feng, B. Jia, C. Zhu, G. An, R. Xiao, X. Feng, Multi-phase field simulation of grain growth in multiple phase transformations of a binary alloy, Chinese Physics B 26(8) (2017).
[171] K. Elder, M. Katakowski, M. Haataja, M. Grant, Modeling elasticity in crystal growth, Phys. Rev. Lett. 88(24) (2002) 245701.
[172] N. Metropolis, A.W. Rosenbluth, M.N. Rosenbluth, A.H. Teller, E. Teller, Equation of State Calculations by Fast Computing Machines, The Journal of Chemical Physics 21(6) (1953) 1087-1092.
[173] M. Anderson, D. Srolovitz, G. Grest, P. Sahni, Computer simulation of grain growth—I. Kinetics, Acta Metall. 32(5) (1984) 783-791.
[174] O. Ivasishin, S. Shevchenko, S. Semiatin, Implementation of Exact Grain-Boundary Geometry Into a 3D Monte-Carlo (POTTS) Model for Microstructure Evolution (Preprint), AIR FORCE RESEARCH LAB WRIGHT-PATTERSON AFB OH MATERIALS AND MANUFACTURING DIRECTORATE, 2008.
[175] J.K. Mason, J. Lind, S.F. Li, B.W. Reed, M. Kumar, Kinetics and anisotropy of the Monte Carlo model of grain growth, Acta Mater. 82 (2015) 155-166.
[176] S. Mishra, T. DebRoy, Measurements and Monte Carlo simulation of grain growth in the heat-affected zone of Ti–6Al–4V welds, Acta Mater. 52(5) (2004) 1183-1192.
[177] P.E. Goins, E.A. Holm, The Material Point Monte Carlo model: A discrete, off-lattice method for microstructural evolution simulations, Computational Materials Science 124 (2016) 411-419.
[178] L. Wang, P. Clancy, Kinetic Monte Carlo simulation of the growth of polycrystalline Cu films, Surf. Sci. 473(1-2) (2001) 25-38.
[179] L. Zhang, A.D. Rollett, T. Bartel, D. Wu, M.T. Lusk, A calibrated Monte Carlo approach to quantify the impacts of misorientation and different driving forces on texture development, Acta Mater. 60(3) (2012) 1201-1210.
[180] D. Tourret, A. Karma, Multi-scale needle-network model of complex dendritic microstructure formation, IOP Conference Series: Materials Science and Engineering 33 (2012).
[181] B. Derrida, V. Hakim, Needle models of Laplacian growth, PhRvA 45(12) (1992) 8759.

Corresponding authors.
E-mail addresses: yaoyao.zhao@mcgill.ca (Y.F. Zhao), bkdzxl@gmail.com (X. Zhou)

[182] D. Tourret, A. Karma, Multiscale dendritic needle network model of alloy solidification, Acta Mater. 61(17) (2013) 6474-6491.
[183] D. Tourret, A.J. Clarke, S.D. Imhoff, P.J. Gibbs, J.W. Gibbs, A. Karma, Three-Dimensional Multiscale Modeling of Dendritic Spacing Selection During Al-Si Directional Solidification, JOM 67(8) (2015) 1776-1785.
[184] J. Liu, Q. Chen, Y. Zhao, W. Xiong, A. To, Quantitative Texture Prediction of Epitaxial Columnar Grains in Alloy 718 Processed by Additive Manufacturing, Proceedings of the 9th International Symposium on Superalloy 718 & Derivatives: Energy, Aerospace, and Industrial Applications, Springer, 2018, pp. 749-755.
[185] L. Costa, R. Vilar, T. Reti, A.M. Deus, Rapid tooling by laser powder deposition: Process simulation using finite element analysis, Acta Mater. 53(14) (2005) 3987-3999.
[186] M.N. Ahsan, A.J. Pinkerton, An analytical–numerical model of laser direct metal deposition track and microstructure formation, Modell. Simul. Mater. Sci. Eng. 19(5) (2011) 055003.
[187] L.E. Criales, Y.M. Arısoy, B. Lane, S. Moylan, A. Donmez, T. Özel, Laser powder bed fusion of nickel alloy 625: experimental investigations of effects of process parameters on melt pool size and shape with spatter analysis, International Journal of Machine Tools and Manufacture 121 (2017) 22-36.
[188] B. Regaard, S. Kaierle, W. Schulz, A. Moalem, Advantages of coaxial external illumination for monitoring and control of laser materials processing, International Congress on Applications of Lasers & Electro-Optics, Laser Institute of America, 2018, p. 2307.
[189] C.L.A. Leung, S. Marussi, R.C. Atwood, M. Towrie, P.J. Withers, P.D. Lee, In situ X-ray imaging of defect and molten pool dynamics in laser additive manufacturing, Nature Communications 9(1) (2018) 1355.
[190] R. Cunningham, C. Zhao, N. Parab, C. Kantzos, J. Pauza, K. Fezzaa, T. Sun, A.D. Rollett, Keyhole threshold and morphology in laser melting revealed by ultrahigh-speed x-ray imaging, Sci 363(6429) (2019) 849-852.
[191] A. Pineau, G. Guillemot, D. Tourret, A. Karma, C.-A. Gandin, Growth competition between columnar dendritic grains–Cellular automaton versus phase field modeling, Acta Mater. 155 (2018) 286-301.
[192] A. Choudhury, K. Reuther, E. Wesner, A. August, B. Nestler, M. Rettenmayr, Comparison of phase-field and cellular automaton models for dendritic solidification in Al–Cu alloy, Computational Materials Science 55 (2012) 263-268.
[193] A. Suárez, M.J. Tobar, A. Yáñez, I. Pérez, J. Sampedro, V. Amigó, J.J. Candel, Modeling of phase transformations of Ti6Al4V during laser metal deposition, Physics Procedia 12 (2011) 666-673.
[194] C.C. Murgau, R. Pederson, L.E. Lindgren, A model for Ti–6Al–4V microstructure evolution for arbitrary temperature changes, Modell. Simul. Mater. Sci. Eng. 20(5) (2012) 055006.
[195] E. Salsi, M. Chiumenti, M. Cervera, Modeling of microstructure evolution of ti6al4v for additive manufacturing, Metals 8(8) (2018) 633.
[196] J. Irwin, E.W. Reutzel, P. Michaleris, J. Keist, A.R. Nassar, Predicting microstructure from thermal history during additive manufacturing for Ti-6Al-4V, Journal of Manufacturing Science and Engineering 138(11) (2016) 111007.
[197] Q. Zhang, J. Xie, Z. Gao, T. London, D. Griffiths, V. Oancea, A metallurgical phase transformation framework applied to SLM additive manufacturing processes, Materials & Design 166 (2019) 107618.
[198] G. Vastola, G. Zhang, Q. Pei, Y.-W. Zhang, Modeling the microstructure evolution during additive manufacturing of Ti6Al4V: a comparison between electron beam melting and selective laser melting, JOM 68(5) (2016) 1370-1375.

Corresponding authors.
E-mail addresses: yaoyao.zhao@mcgill.ca (Y.F. Zhao), bkdzxl@gmail.com (X. Zhou)

[199] L.E. Lindgren, A. Lundbäck, M. Fisk, R. Pederson, J. Andersson, Simulation of additive manufacturing using coupled constitutive and microstructure models, Additive Manufacturing 12 (2016) 144-158.

Corresponding authors.
E-mail addresses: yaoyao.zhao@mcgill.ca (Y.F. Zhao), bkdzxl@gmail.com (X. Zhou)